ACS Infectious Diseases

pubs.acs.org/journal/aidcbc

Article

Pharmacokinetic/Pharmacodynamic Determination and Preclinical Pharmacokinetics of the β-Lactamase Inhibitor ETX1317 and Its Orally Available Prodrug ETX0282

John O'Donnell,* Angela Tanudra, April Chen, Daniel Hines, Ruben Tommasi, and John Mueller

Cite This: *ACS Infect. Dis.* 2020, 6, 1378−1388

Read Online

ACCESS | Metrics & More | Article Recommendations | Supporting Information

ABSTRACT: Increasingly resistant Enterobacteriaceae have emerged as a health threat in both hospital and community settings. Infections of the urinary tract, once often treated with oral agents in the community, are requiring increased hospitalization and use of intravenously administered agents for effective treatment. These isolates often carry extended spectrum β-lactamases (ESBLs) and carbapenemases that necessitate the need for an inhibitor to cover a broad range of β-lactamases. ETX1317 is a novel diazabicyclooctane class serine β-lactamase inhibitor that restores the antibacterial activity of several classes of β-lactams, including third-generation cephalosporins such as cefpodoxime. ETX1317 is currently being developed as an orally available prodrug, ETX0282, to be administered with cefpodoxime proxetil (CPDP). The combination has demonstrated oral efficacy in murine models of infection. Pharmacokinetics established in preclinical species and pharmacokinetic/pharmacodynamic attributes suggest the orally administered combination ETX0282 + CPDP could serve as an effective treatment option against contemporary ESBL and carbapenemase-producing *Enterobacteriaceae*.

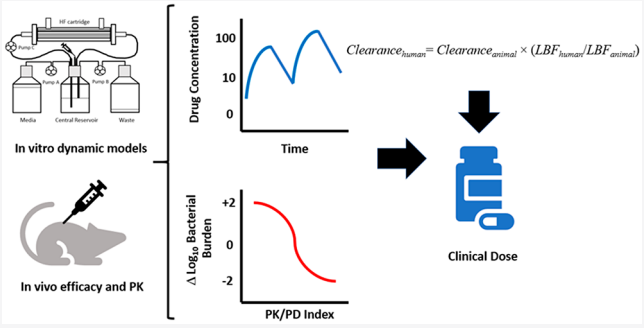

KEYWORDS: *Enterobacteriaceae, β-lactamase inhibitor, diazabicyclooctanes, pharmacokinetics, PK/PD, oral bioavailability*

Increased prevalence of extended spectrum β-lactamase (ESBL)-producing and carbapenem-resistant Enterobacteriaceae (CRE) has led to a shortage of effective agents to treat infections that were once readily susceptible to multiple classes of antibiotics.[1−3] Urinary tract infections (UTIs), previously often treated effectively in an outpatient setting with fluoroquinolones, are now becoming increasingly drug resistant, leading to higher hospitalization rates.[4,5] A distinct advantage of fluoroquinolones was their use as oral agents, allowing convenient administration. Fluoroquinolone resistance observed in Gram-negative UTI isolates, however, is now in excess of 40% in some geographic regions.[6,7] In one hospital, resistance to levofloxacin increased nearly 10-fold over a period of only 6 years.[8] Newly developed β-lactamase inhibitors exhibiting broad spectrum activity are showing promise; however, their use is primarily restricted to intravenous administration.[9] The convenience of oral administration would be particularly valuable in a setting of an oral step-down therapy after initial parenteral administration to reduce hospital stays or potentially to treat orally outside of the hospital altogether.

Within the β-lactam (BL) class of compounds, penicillins such as ampicillin and amoxicillin have historically been broadly utilized against a variety of Gram-positive and Gram-negative pathogens.[10,11] As resistance to these agents has emerged in the form of an increased spectrum of β-lactamase activity, the addition of a β-lactamase inhibitor (BLI) has extended the utility of these compounds. For instance, the addition of sulbactam to ampicillin resulted in the intravenously (i.v.) administered product ampicillin/sulbactam injection, which still maintains a viable market share today.[12] The oral availability of clavulanate has extended its use beyond i.v. administration. Pairing clavulanate with amoxicillin resulted in the discovery of oral amoxicillin/clavulanate, which has maintained broad use in the community setting.[13] Recognition of amoxicillin as a substrate for the active transporter PEPT1,[14] which is expressed in the GI tract, is thought to be responsible for its relatively high bioavailability in excess of 70%. These early BL/BLI combinations were quite effective, but their widespread use ultimately led to the emergence of broader spectrum classes of β-lactamases that are not readily inhibited by first-generation inhibitors like clavulanate. Modification of

Special Issue: Antibiotics

Received: January 15, 2020
Published: May 7, 2020

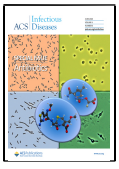

the BL ring and consideration of other related classes such as cephalosporins have helped circumvent some of the substrate affinity of these contemporary classes of β-lactamases, but as more frequent use prevailed, so did the evolution of ESBLs.[15−17] Approaching the problem more recently with the discovery and development of β-lactamase inhibitors that provide inhibitory potency against multiple classes of β-lactamases has led to the advancement of several new classes of inhibitors such as diazabicyclooctanes, which include the BLI avibactam,[18] and cyclic boronates, such as vaborbactam.[19] These contemporary inhibitors have demonstrated favorable inhibition against ESBL and carbapenemase-producing Gram-negative pathogens, but they are currently limited to i.v. dosing—often requiring prolonged infusion via multiple administrations per day. While this is adequate for use in the hospital, oral administration provides an opportunity to reduce hospital stays with post-i.v. to oral step-down therapy or oral use outside of the hospital altogether.[20] Two significant hurdles, however, have limited the successful discovery of orally active contemporary BL/BLI combinations: (1) physicochemical properties consistent with favorable oral absorption and/or structural features lending to the ability to prodrug the molecule and (2) limited options of orally active BLs or cephalosporins to match with these inhibitors.

ETX0282 is an orally available ester prodrug of the novel β-lactamase inhibitor ETX1317 (Figure 1). ETX1317 is a diazabicyclooctane class inhibitor with broad inhibition of class A, C, and D serine β-lactamases, including ESBL and carbapenemase-producing Enterobacteriaceae as well as fluoroquinolone-resistant isolates.[21] Minimum inhibition concentration (MIC) testing of ETX1317 in combination with previously approved BLs and cephalosporins has recently been completed with an emphasis on finding effective oral combinations.

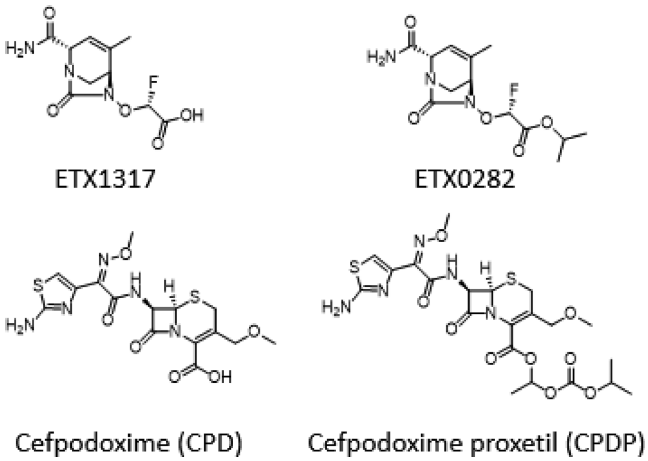

Figure 1. Structures of ETX1317, ETX0282, cefpodoxime (CPD), and cefpodoxime proxetil (CPDP).

The present study identifies the pharmacokinetic/pharmacodynamic (PK/PD) index of ETX1317 and exposure magnitudes associated with *in vitro* and *in vivo* efficacy against clinically relevant isolates when used in combination with cefpodoxime. The selection of cefpodoxime as the optimum combination partner is also presented in consideration of MIC, approved clinical dosing of its oral prodrug ester cefpodoxime proxetil (CPDP), and unbound exposure. Pharmacokinetic studies in preclinical species were used to project ETX0282 and ETX1317 PK in humans. These data were used in combination with *in vitro* PK/PD evaluations and oral efficacy studies in mice to estimate effective clinical doses in patients.

RESULTS AND DISCUSSION

Selection of β-Lactam (Antibiotic) Partner. Previously approved penicillins and cephalosporins administered orally have been evaluated in combination with ETX1317 against broad panels of contemporary Enterobacteriaceae strains which express ESBLs and carbapenemases.[21] While MIC potency in the presence of ETX1317 was the primary selection criterion, high bioavailability, approved dose levels, and unbound exposure achieved were also important considerations. Nearly all contemporary cephalosporins demonstrate high urinary excretion, which is important for treating UTIs.[22] Cefpodoxime (CPD) emerged as a lead candidate based upon its approved use as an orally available proxetil ester prodrug ($F\% \approx 50\%$ at a top dose of 400 mg q12h (800 mg/day), translating to mean unbound concentrations exceeding at least 0.5 μg/mL for greater than 50% of the dosing interval).[23,24] As unbound concentrations drive efficacy in tissues, protein binding must be considered in the context of bloodstream and tissue-based infections. CPD target exposure was based upon published PK/PD for BLs and, more specifically, third-generation cephalosporins such as CPD. Those papers have shown in preclinical models of infection that efficacy is achieved with cephalosporins when unbound drug concentrations exceed the MIC for 50% or higher of the dosing interval ($fT > MIC \geq 50\%$). This is the case for not only parenteral cephalosporins but oral agents as well, such as CPDP.[25,26] An important observation in these studies was that the PK/PD driver and magnitude do not change with resistance phenotype. Both ESBL producers and non-ESBL producers achieve similar dose responses relative to their MICs. Against both ESBL- and non-ESBL-producing organ-

Table 1. MICs of Enterobacteriaceae Strains Used for PK/PD Studies

isolate	β-lactamase content	MIC (μg/mL)		
		ETX1317[b]	cefpodoxime	cefpodoxime-ETX1317 (1:2)
K. pneumoniae ARC4488	SHV-11, CTX-M-15, OXA-1, TEM-1	0.5	>64	0.25
K. pneumoniae ARC4486	OXA-1 [E69K], DHA-1, SHV-11	32	>64	0.25
E. coli ARC2687	AmpC, CTX-M-14	0.5	>64	0.125
K. pneumoniae ARC5118	SHV-5, TEM-1, KPC-3	32	>64	1
K. pneumoniae ARC4420	SHV-12, OXA-1, DHA-1, SHV-11	16	>64	1
E. coli ARC4419	AmpC, SHV-12	0.25	64	0.125
E. coli NMC101[a]	AmpC, CTX-M-14	1	>64	0.125

[a]Mutations associated with ETX1317 resistance are CysE [del A204-A222] and ttcA [T134aA]. [b]MIC_{BLI}.

https://dx.doi.org/10.1021/acsinfecdis.0c00019
ACS Infect. Dis. 2020, 6, 1378−1388

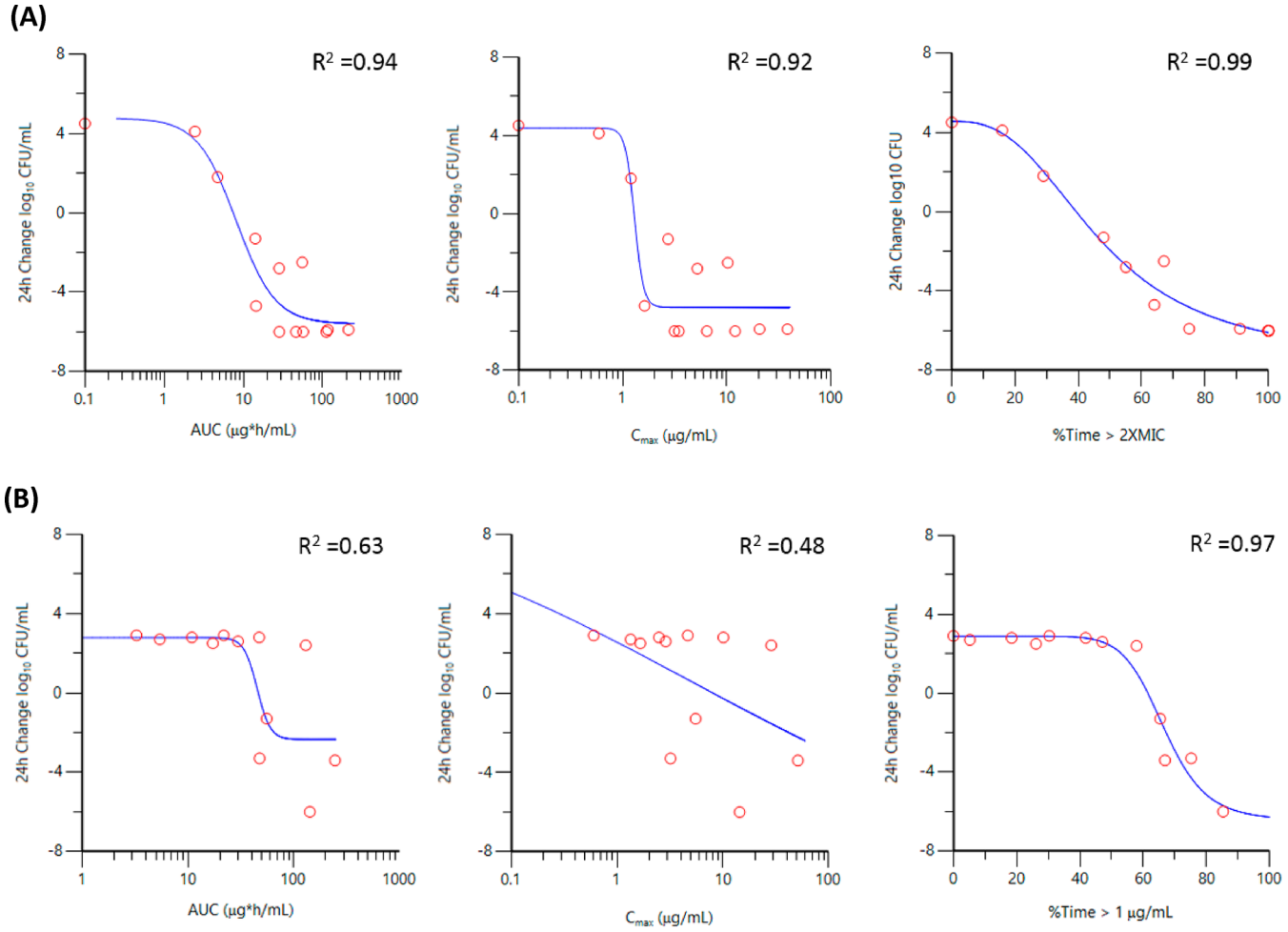

Figure 2. C_{max}, AUC, and %Time > critical threshold (C_T) of ETX1317 vs 24 h change $\log_{10}$ CFU/mL versus *E. coli* ARC2687 in hollow-fiber model (A) and *K. pneumoniae* ARC4420 in chemostat model (B).

Table 2. Correlation Coefficient (R^2) of PK/PD Index to Observed Activity of ETX1317

PK/PD index	Eco ARC2687[a]	Kpn ARC4486[a]	Kpn ARC4488[a]	Kpn ARC5118[b]	Kpn ARC4420[b]
AUC	0.94	0.91	0.93	0.72	0.63
C_{max}	0.92	0.80	0.83	0.51	0.48
C_T 0.5× MIC	0.96	0.91	0.87	0.92	0.94
C_T 1.0× MIC	0.96	0.95	0.92	0.97	0.97
C_T 2.0× MIC	0.99	0.96	0.99	0.86	0.78

[a]*In vitro* dynamic study utilizing hollow-fiber infection model. [b]*In vitro* dynamic study utilizing chemostat model.

isms, PK/PD endpoints of stasis (no net change in $\log_{10}$ CFU over 24 h of therapy), a net 1−$\log_{10}$ CFU reduction (1−log kill), and maximal efficacy were associated with fT > MIC of 40, 50, and 60% of the dosing interval, respectively. As a PK/PD endpoint of 1−log kill was targeted, CPD fT > MIC of 50% was considered throughout all *in vitro* and *in vivo* experiments conducted in the present study.

MIC Determination of Enterobacteriaceae Isolates for PK/PD Studies. MICs were determined utilizing a 1:2 ratio of cefpodoxime:ETX1317. This methodology of ratio testing, as opposed to titrating the BL in the presence of a constant concentration of the BLI, was found to be optimal when the BLI demonstrates intrinsic activity.[27] The isolates utilized in the present study (Table 1) were broadly insensitive to CPD, presumably due to the presence of ESBLs and carbapenemases expressed in these strains. The addition of ETX1317 restored CPD activity to ≤1 μg/mL across all the tested isolates.

PK/PD Driver Determination in Hollow-Fiber and Chemostat Models. The PK/PD driver of ETX1317 was assessed in the presence of CPD in both hollow-fiber[28−31] and chemostat[32] *in vitro* infection model systems. In all cases, CPD was administered q12h via a 2 h infusion and eliminated with a 2 h half-life, with the concentration of drug exceeding the MIC (the MIC of CPD in the presence of ETX1317 at a 1:2 ratio) for 50% of the dosing interval for each strain. Representative E_{max} plots are shown graphically for *Escherichia coli* ARC2687 in the hollow-fiber model and *Klebsiella pneumoniae* ARC4420 in the chemostat system (Figure 2). As summarized in Table 2, the PK/PD of ETX1317 showed time dependence with % Time > a critical threshold (C_T), demonstrating superior correlation to activity relative to pharmacokinetic parameters

https://dx.doi.org/10.1021/acsinfecdis.0c00019
ACS Infect. Dis. 2020, 6, 1378−1388

C_{max} and AUC. This was more apparent in the chemostat model vs *K. pneumoniae* ARC4420 and ARC5118 which demonstrated higher MICs of 1 μg/mL in the presence of ETX1317. This could partially be attributed to the distribution of the concentration ranges utilized for the hollow-fiber infection model (HFIM) where most of the data scatter occurred in the efficacious dose range for lower MIC strains. It is important to note that initial evaluation of *K. pneumoniae* ARC4420 and ARC5118 was completed in the HFIM but rapid degradation of CPD, presumably through accumulation of β-lactamases in the extra-capillary space of the cartridge precluded a reliable assessment of the PK/PD driver with these strains in this model.[32] Other investigators have also suggested β-lactamase accumulation as a potential issue in the HFIM.[29,33] In both the HFIM and chemostat models the optimum critical threshold of ETX1317 was established through iterative E_{max} fitting of a range of ETX1317 concentrations from 0.5× to 2× the CPD:ETX1317 MIC value. In the HFIM, %Time > ETX1317 C_T of 2× MIC provided the highest correlation to observed activity which appeared to be independent to the apparent intrinsic activity of ETX1317 (as reflected by ETX1317 MIC_{BLI} of *K. pneumoniae* ARC4486 vs ARC4488). Interestingly for *K. pneumoniae* ARC4420 and ARC5118 exhibiting higher a MIC of 1 μg/mL, a C_T of 1× MIC provided the best correlation in the chemostat system. In both models CPD infused alone mimicked vehicle control as expected with similar growth of +2 to 4 $\log_{10}$ CFU/mL. Unexpectedly infusion of ETX1317 alone q12h to a C_{max} of 16 μg/mL resulted in +0.5 log growth despite achieving 100%Time > the ETX1317 MIC_{BLI} exposure suggesting the apparent intrinsic antibacterial activity of the inhibitor does not translate to cidal activity on its own.

PK/PD-derived exposure targets for BLIs have utilized various approaches for clinical dose setting. The use of a singular critical threshold value independent of MIC has been used for recent BL/BLI combinations such as ceftazidime/avibactam[34] aztreonam/avibactam,[35] but this has been problematic to correlate activity across a broad range of MICs. More recent work with ceftolozane/tazobactam[36] and other BLI combinations[37,38] considers a critical threshold value that varies proportionally to the MIC value. More BLI is obviously required for inhibition of bacterial growth in strains exhibiting higher expression of β-lactamases and where β-lactamase production is the primary resistance determinant.[36] As shown in Table 3, the use of a singular ETX1317 critical threshold value of 1 μg/mL provided an excellent correlation to activity in both the hollow-fiber and chemostat models across the MIC range of 0.125−1 μg/mL, but decreased susceptibility led to a shift in the dose response curves in order to achieve PK/PD endpoints of stasis and 1−log kill. Alternately, a reasonable fit of the data (R^2 = 0.87) is achieved across all strains when activity is correlated to %Time > ETX1317 C_T of 2× MIC (Figure 3). Convergence of the data to a threshold value related to MIC simplifies dose setting and, in this case, appears to be consistent across a broad range of susceptibility (0.125−1 μg/mL).

Oral Efficacy of ETX0282 Combined with CPDP *In Vivo*. All *in vivo* efficacy studies were supported with PK of ETX1317 and CPD following oral administration of ETX0282 and CPDP. For the purposes of understanding the exposure-PD response relationship, total systemic concentrations of ETX1317 and cefpodoxime were normalized to unbound drug levels after accounting for protein binding with percent unbound estimates of 93% and 66%, respectively, in mouse plasma (Table S2). An *in vivo* dose range study with CPDP administered alone against a susceptible *E. coli* strain (ATCC 25922, CPD MIC = 0.5 μg/mL) was completed initially in a murine neutropenic thigh model to confirm its PK/PD target. In this study a 50 mg/kg oral dose of CPDP administered q6h was consistent with achieving 1−log kill over 24 h. Unbound concentrations at this dose were above the MIC for ∼50% of the dosing interval, consistent with exposure for cephalosporins to achieve cidal activity.[39,40] The oral dose combination of CPDP and ETX0282 demonstrated robust *in vivo* efficacy in a murine neutropenic thigh infection model against CPD resistant strains. The %Time > unbound concentrations of ETX1317 across the dose range of the studies are summarized in Table 4. No concentrations of intact CPDP and ETX0282 were observed systemically suggesting rapid conversion of both prodrug esters once absorbed in mice. Oral exposure was generally dose proportional to 50 mg/kg; however, it became less than dose proportional at ≥200 mg/kg.

The change in bacterial burden over 24 h as a function of dose against *E. coli* ARC2687, *K. pneumoniae* ARC4488, and *K. pneumoniae* ARC5118 is summarized in Table 5. Box-Whisker plots of the individual data are provided in Figure S2. Administration of CPDP or ETX0282 alone demonstrated no significant reduction in CFU counts and generally mimicked vehicle control (+2.5 to +4 $\log_{10}$ CFU/g). Meropenem dosed subcutaneously at a 600 mg/kg dose q6h was used as a comparator control. *E. coli* ARC2687 and *K. pneumoniae* ARC4488 are ESBL producers but maintain susceptibility to meropenem. *K. pneumoniae* ARC5118 is a KPC-producing isolate and is resistant to meropenem. As expected, cidal activity (≥1 $\log_{10}$ CFU/g reduction achieved in 24 h) was observed with meropenem against *E. coli* ARC2687 but not against *K. pneumoniae* ARC5118. Consistent with achieving unbound ETX1317 exposures at or above the PK/PD endpoint of 2× MIC, cidal activity was observed for the CPDP:ETX0282 combination against *E. coli* ARC2687 at 24 h post initiation of therapy.

In vitro hollow-fiber and chemostat experiments conducted with CDP and ETX1317 demonstrated that unbound ETX1317 concentrations in excess of 2× MIC for 50% of the dosing interval were associated with reducing bacterial burden below stasis. The *in vivo* activity of CPDP:ETX0282

Table 3. %Time > C_T of 1 μg/mL of ETX1317 to Meet PK/PD Endpoints in the *In Vitro* Hollow Fiber and Chemostat Models

strain	MIC[a] (μg/mL)	model[b]	%Time > C_T of 1 μg/mL		
			R^2	stasis	1−$\log_{10}$ kill
E. coli ARC2687	0.125	HFIM	0.96	7%	14%
K. pneumoniae ARC4486	0.25	HFIM	0.96	37%	49%
K. pneumoniae ARC4488	0.25	HFIM	0.99	43%	47%
K. pneumoniae ARC4420	1	chemo	0.97	59%	63%
K. pneumoniae ARC5118	1	chemo	0.97	60%	65%

[a]MIC of CPD in the presence of ETX1317 at a 1:2 ratio CPD:ETX1317. [b]chemo = chemostat; HFIM = hollow fiber infection model.

https://dx.doi.org/10.1021/acsinfecdis.0c00019
ACS Infect. Dis. 2020, 6, 1378−1388

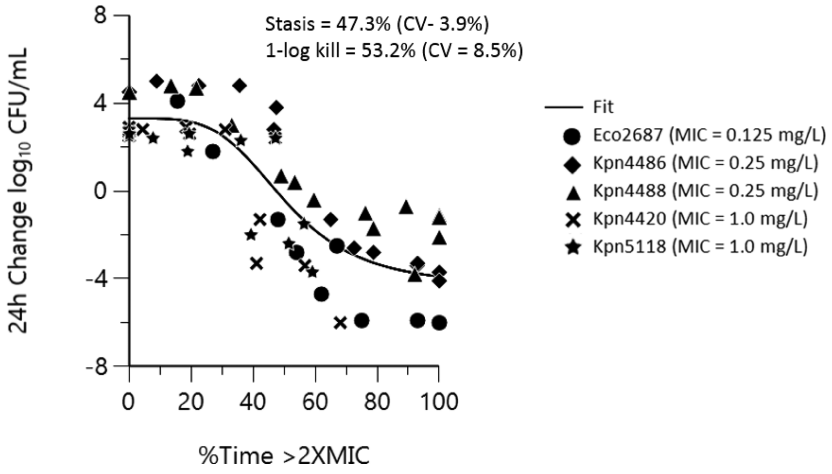

Figure 3. Combined strain E_{max} plot of %Time > 2× MIC vs 24 h change $\log_{10}$ CFU/mL (R^2 = 0.87).

Table 4. Unbound Exposure of EXT1317 Following Oral Administration of ETX0282

			%Time > f[CT][a]			
dose (mg/kg)	fC_{max} (μg/mL)	$fAUC_{last}$ (μg hr/mL)	0.25 μg/mL	0.5 μg/mL	1.0 μg/mL	2.0 μg/mL
10	3.9	4.7	47	25	12	8
50	21	23	88	50	29	28
200	57	61	100	100	58	35
400	90	73	100	100	75	38

[a]ETX1317 is 93% unbound in mouse plasma.

Table 5. *In Vivo* Efficacy of Cefpodoxime Proxetil ± ETX0282 Following Oral Administration in a Murine Neutropenic Thigh Study[a]

			$\log_{10}$ CFU/g thigh change 24 h post therapy initiation		
group	dose (mg/kg)	regimen	Eco ARC2687 MIC = 0.125 μg/mL[b]	Kpn ARC4488 MIC = 0.25 μg/mL[b]	Kpn ARC5118 MIC = 1.0 μg/mL[b]
infection control	vehicle	p.o./q6h	+4.23	+4.12	+2.57
CPDP only	50	p.o./q6h	+3.61	+3.58	+2.66
ETX0282 only	50	p.o./q6h	+2.93[c]	ND	+1.31
CPDP:ETX0282	50:10	p.o./q6h	−0.86	+0.74	+1.16
	50:50	p.o./q6h	−1.04[d]	−0.18	+0.30
	50:200	p.o./q6h	−1.11[e]	−0.43	−0.31
	50:400	p.o./q6h	ND	ND	−0.38
meropenem	600	s.c./q6h	−1.46	ND	+2.04

[a]Abbreviations: CFU = colony forming units; CPDP = cefpodoxime proxetil; ND = not done; p.o. = oral; q6h = every 6 h; s.c. = subcutaneous. [b]Strain and CPD:ETX1317 (1:2) MIC. [c]10 mg/kg ETX0282 vs ARC2687. [d]50:25 mg/kg CPDP:ETX0282 vs ARC2687. [e]50:100 mg/kg CPDP:ETX0282 vs ARC2687.

Table 6. *In Vivo* Efficacy of ETX0282 Alone and in Combination with Cefpodoxime Proxetil against Strains Demonstrating ETX1317 Intrinsic Activity[a]

			$\log_{10}$ CFU/g thigh change 24 h post therapy initiation	
group	dose (mg/kg)	regimen	Eco NMC101 MIC = 1 μg/mL[b]	Eco ARC4419 MIC = 0.25 μg/mL[b]
infection control	vehicle	p.o./q6h	+3.64	+2.52
CPDP only	50	p.o./q6h	+3.39	+2.23
ETX0282 only	10	p.o./q6h	+2.10	+1.41
ETX0282 only	50	p.o./q6h	+1.83	+1.06
ETX0282 only	200	p.o./q6h	+1.39	+1.07
CPDP:ETX0282	50:10	p.o./q6h	ND	−1.23
	50:50	p.o./q6h	−1.13	−1.39
	50:200	p.o./q6h	ND	−1.37
meropenem	600	s.c./q6h	−1.36	−2.19

[a]Abbreviations: CFU = colony forming units; CPDP = cefpodoxime proxetil; ND = not done; MIC = minimum inhibitory concentration; p.o. = oral; q6h = every 6 h; s.c. = subcutaneous. [b]Strain and ETX1317 MIC_{BLI}.

https://dx.doi.org/10.1021/acsinfecdis.0c00019
ACS Infect. Dis. 2020, 6, 1378−1388

Table 7. Pharmacokinetics of ETX1317 Following Intravenous Administration to Rats, Dogs, and Monkeys[a]

species	dose (mg/kg)	C_{max} (μg/mL)	AUC (μg·h/mL)	$T_{1/2}$ (h)	$V_{d,ss}$ (L/kg)	CL (mL/min/kg)	renal CL (mL/min/kg)
rat	10	17.5 ± 2.0	7.19 ± 0.34	0.4 ± 0.02	0.70 ± 0.01	23.1 ± 1.1	13.4 ± 0.3
dog	1	2.27 ± 0.49	2.76 ± 0.34	0.8 ± 0.1	0.38 ± 0.05	5.7 ± 0.7	1.1 ± 0.3
monkey	0.87	3.12 ± 0.23	2.68 ± 0.21	1.1 ± 0.1	0.31 ± 0.02	5.7 ± 0.7	2.2(1.3−3.6)

[a]Abbreviations: AUC = area under the curve; CL = clearance; C_{max} = peak concentration; $T_{1/2}$ = half-life; $V_{d,ss}$ = volume of distribution at steady state.

against *K. pneumoniae* ARC4488 and ARC5118 was generally consistent with *in vitro* data generated for these strains, although a 1−log kill was not achieved.

Oral *In Vivo* Efficacy of ETX0282 against Strains Demonstrating ETX1317 Intrinsic Activity *In Vitro*. As shown in Table 1, some isolates demonstrated susceptible MICs to ETX1317 alone (referred to as MIC_{BLI} for clarity), suggesting intrinsic activity of the BLI. To further understand whether this *in vitro* activity translated to *in vivo* efficacy, an additional neutropenic thigh study was conducted in mice with increasing doses of ETX0282 alone vs *E. coli* NMC101 (ETX1317 MIC_{BLI} = 1 μg/mL) and ARC4419 (ETX1317 MIC_{BLI} = 0.25 μg/mL). As shown in Table 4, at the top dose of 200 mg/kg, unbound ETX1317 concentrations exceed a concentration of 1 μg/mL for 58% of the dosing interval and 100% of the dosing interval at a concentration of 0.25 μg/mL. Despite the significant exposure of ETX1317, a 200 mg/kg q6h dose of ETX0282 alone was ineffective for both strains (Table 6). However, when CPDP was added at a dose level of 50 mg/kg in combination with ETX0282 at a dose level of 50 mg/kg administered q6h, cidal activity was achieved for both strains. This would be anticipated, as the 50:50 mg/kg CPDP:ETX0282 q6h dose level exceeds the PK/PD exposure requirements of 50%Time > MIC for CPD and 60%Time > 2× MIC (CPD:ETX1317 MICs of 0.125 mg/L for both strains). It is clear from these investigations that antibacterial potency of ETX1317 due to apparent intrinsic activity of the molecule is not representative of robust cidal activity *in vivo*, and efficacy is only realized with the combination of CPDP and ETX0282—a finding that has been observed in recent studies with β-lactamase inhibitors.[41]

Preclinical PK of ETX1317 (i.v.) and ETX0282 (p.o.) in Mice, Rats, Dogs, and Monkeys. Intravenous and oral pharmacokinetics of ETX1317 and ETX0282 in preclinical species are summarized in Table 7 and Table S1, respectively. Time vs concentration profiles are depicted graphically in Figure S1. Oral administration of the ester prodrug ETX0282 at doses ranging from 1 to 10 mg/kg in rats, dogs, and monkeys resulted in circulating concentrations of ETX1317 with minimal to no levels of ETX0282, suggesting rapid and complete conversion upon absorption and first-pass metabolism. These observations were consistent with *ex vivo* liver S9 incubations with ETX0282, suggesting efficient conversion across all species, including humans.[42] Once formed, ETX1317 was eliminated with a half-life of 1.3 h in mice, 0.4 h in rats, 0.8 h in dogs, and 1.1 h in monkeys. ETX1317 protein binding was very low, with the fraction unbound ranging from 0.77 to 1.0 across monkeys, humans, mice, rats, and dogs, and was found to be consistent across a concentration range from 1 to 100 μM (Table S2).

In rats, mean total clearance of 23 mL/min/kg and steady-state volume of distribution of 0.70 L/kg were determined following i.v. administration of ETX1317. Comparison of ETX1317 AUCs after i.v. dosing of ETX1317 and oral dosing of ETX0282 suggested oral bioavailability of 98%. Similar to rats, oral bioavailability in dogs was 97%, suggesting high absorption and efficient conversion of ETX0282 in this species. Mean ETX1317 clearance of 5.7 ± 0.7 mL/min/kg and a mean volume of distribution 0.38 ± 0.05 L/kg were estimated following i.v. administration to dogs. In monkeys a mean clearance of 5.7 ± 0.7 mL/min/kg and a mean volume of distribution of 0.31 ± 0.02 L/kg were determined for ETX1317. Renal clearance based upon excretion of ETX1317 in the urine was nearly 40% of total clearance (range 23−63%). Oral bioavailability was also high in monkeys, with an estimate of 78%. Oral bioavailability was not estimated in mice as no i.v. dose of ETX1317 was administered to this species.

ETX1317 Human PK Prediction. The methodology utilized for prediction of human PK of ETX1317 was consistent with methods used in support of similar chemotypes such as avibactam and ETX2514.[43] Human predictions for volume of distribution ($V_{d,ss}$) and clearance (CL) were within 2-fold of observed mean data obtained in Phase 1 studies, with renal clearance as the predominant clearance mechanism.[44,45] Pharmacokinetic and excretion data from rats, dogs, and monkeys were used collectively for the projection of ETX1317 PK. Liver S9 incubations were also performed across all species (including human) to confirm consistent conversion of ETX0282 to ETX1317 at projected dose levels of ETX0282.[42] Human PK prediction of ETX1317 was completed using single species allometry for volume of distribution from dog PK and dog and monkey single species scaling using liver blood flow to predict non-renal clearance (CL_{NR}).[46] Renal excretion of unchanged drug was found to be a significant route of elimination across all species. While urinary excretion of ETX1317 was lower in dogs relative to monkeys and rats, human renal clearance (CL_R) was predicted using dog-human renal correlation,[47] as this method has been highly predictive for compounds that are generally eliminated via renal excretion. The elimination half-life was estimated based upon the combined use of predicted parameters for clearance and volume of distribution, where $T_{1/2}$ = ln 2*$V_{d,ss}$/CL_{total}. Allometric scaling predicted human $V_{d,ss}$ of 0.35 L/kg. Renal clearance (CL_R) was predicted as 0.74 mL/min/kg using the dog-human renal correlation. Using non-renal clearance in dogs and monkeys, scaling by liver blood flow predicted non-renal clearance in humans of 2.65 and 1.77 mL/min/kg, respectively. Thus, projected total clearance (CL_T), where CL_T = CL_R + CL_{NR}, ranged from 2.51 to 3.39 mL/min/kg, suggesting a half-life of 1.2−1.6 h.

ETX0282 Oral Bioavailability Prediction in Humans. Low-dose oral PK of ETX0282 in rats, dogs, and monkeys demonstrated high bioavailability, ranging from 78% to 98%. Good stability of ETX1317 in liver microsomes and high bioavailability across multiple species suggests that first-pass loss of ETX1317 is not significant upon absorption of ETX0282. Extensive and quantitative conversion of

https://dx.doi.org/10.1021/acsinfecdis.0c00019
ACS Infect. Dis. 2020, 6, 1378−1388

ETX0282 to ETX1317 in liver S9, along with minimal excretion of ETX1317 into the bile, also supports the projection of minimal first-pass losses. Based upon the nonclinical PK data, a range of 60−80% bioavailability and a moderate absorption rate of 0.5−1.0 h^{-1} have been considered for humans. In consideration of these predicted parameters, mean percent fT > C_T of 1 μg/mL (2× MIC of 0.5 μg/mL) estimates for a 500 mg ETX1317 equiv q12h dose of ETX0282 are summarized in Table S3.

CONCLUSIONS

An increase in Enterobacteriaceae resistance due to ESBL- and carbapenemase-producing isolates has led to the recent development of novel BLIs with a broader coverage against multiple classes of β-lactamases. Unfortunately, very few contemporary BL/BLI combinations are suitable for oral administration. The combination of ETX0282 and CPDP shows favorable attributes for the potential treatment of these pathogens in and outside of the hospital setting. PK/PD evaluation in both *in vitro* dynamic model systems and *in vivo* models of infection suggest the combination would be expected to demonstrate cidal activity when unbound exposures of CPD exceed 50%Time > MIC and ETX1317 exceeds a concentration 2× the MIC for 60% of the dosing interval. High bioavailability and complete conversion of ETX0282 to ETX1317 systemically have been demonstrated across multiple preclinical species. Allometric scaling of animal PK suggests clinical kinetics of ETX1317 would behave similarly to cefpodoxime, allowing for fixed-combination oral dosing of ETX0282 and CPDP.

METHODS

Susceptibility Studies. The MIC of each isolate was determined using the broth microdilution method following CLSI guidelines of document M07-A7 (CLSI M07-A7).

Hollow-Fiber and Chemostat Inoculum Preparation. Enterobacteriaceae isolates *E. coli* ARC2687 and *K. pneumoniae* isolates ARC4486, ARC4488, ARC5118, and ARC4420 were prepared for infection from an overnight plate culture. On the day of the experiment, a few colonies of bacteria were inoculated in Mueller Hinton Broth II (MHBII, Sigma-Aldrich, St. Louis, MO) and incubated at 35 °C until reaching log-phase growth, about 1 h. In hollow-fiber studies cell population density is confirmed by turbidimetric assay (OD_{600}) and final dilution is adjusted to deliver approximately 15 mL of bacteria (1×10^6 CFU/mL) to the extra-capillary space of the hollow-fiber cartridge (Fibercell Systems, Inc., Frederick, MD). After 1 h, targeted drug concentrations were introduced using a 2 h infusion via a syringe pump (Harvard Apparatus, Holliston, MA). For chemostat experiments approximately 1 mL of bacteria (1×10^8 CFU/mL) were introduced to the chemostat reservoir bottle with 100 mL MHBII to dilute bacterial culture and reach a target CFU density of 1×10^6 CFU/mL. After 5 min, each chemostat bottle was exposed to targeted drug with a 2 h infusion administered via syringe pump.

***In Vitro* Test Article Formulation.** ETX1317 and CPD were dissolved in MHBII (accounting for potency) and delivered as a 2 h infusion via syringe pump (Harvard Apparatus, Holliston, MA). Solubility and stability were confirmed at room temperature for the experiment. Dose formulation potency was verified by LC/MS/MS.

Hollow-Fiber and Chemostat Study Designs. Dose range and dose fractionation were performed in hollow-fiber infection model (HFIM) and chemostat (one-compartment) *in vitro* infection model. Bacteria treated with media only (growth control) and dose arms spanning a 64-fold exposure range of drug delivered within regimens of q6h, q12h, and q24h were used. *E. coli* ARC2687 and *K. pneumoniae* ARC4486 and ARC4488 were completed in the HFIM. *K. pneumoniae* ARC5118 and ARC4420 were studied in the chemostat system. CPD concentrations were targeted to achieve exposure of ∼50%Time > MIC determined in the presence of ETX1317. Both CPD and ETX1317 were administered via a 2 h infusion from syringe pumps (Harvard Apparatus) to mimic the approximate C_{max} following oral absorption observed clinically for CDP. The PK profiles for both CPD and ETX1317 were controlled by infusion of the compounds and dilution of media in the central compartment reservoir. Once infused, drug concentration in the HFIM was eliminated by isovolumetrically replacing drug-containing medium with drug-free medium using digital pumps simulating a half-life of 2 h, which is the half-life of CPD in humans. While these parameters nearly replicate PK of CPD clinically in a BID (q12h) regimen over 24 h, the dose of CPD is adjusted to deliver the required 50%Time > MIC concentrations of CPD relative to each isolate's MIC. This regimen would serve as the background exposure of CPD during the dose fractionation of ETX1317. The daily doses of ETX1317 were fractionated via once daily (q24h), every 12 h (q12h), or every 6 h (q6h) to vary the ETX1317 AUC, C_{max}, and %Time > C_T across the dose arms. The system simulated a single compartment PK model with monoexponential elimination of both ETX1317 and CPD. The experiment was maintained at 35 °C in a humidified incubator for the duration of the study. Bacterial burden (CFU/mL) was serially assessed by sampling (500 μL) from the extra-capillary space of the HFIM cartridge at predetermined time points. Serial PK samples (500 μL) were also collected over 24 h time period to ascertain drug exposure. Bacterial samples were diluted (serial 10-fold dilutions), plated on blood agar plates (Remel, Lenexa, KS), and incubated at 35 °C overnight, and colony forming units (CFUs) were enumerated visually.

Animal Welfare Statement. All *in vivo* procedures were completed in compliance with the Animal Welfare Act Regulations (9 CFR 3) under Entasis reviewed IACUC protocols and under the supervision of a site attending veterinarian.

***In Vivo* Thigh Infection Model.** *In vivo* neutropenic infection models in the mouse were conducted as previously described.[48,49] All procedures were performed to Entasis approved IACUC policies and guidelines as well as OLAW standards. Briefly, Female CD-1 mice (20−22 g, Charles River Laboratories) were acclimated for 5 days prior to start of study. Animals were housed 3 per cage with free access to food and water. Mice were rendered neutropenic via two doses of cyclophosphamide on days −4 and −1 with 150 mg/kg and 100 mg/kg delivered intraperitoneally in a dose volume of 10 mL/kg, respectively.[48]

Enterobacteriaceae isolates ARC2687, ARC4488, ARC5118, NMC101, and ARC4419 were prepared for infection from an overnight plate culture. A portion of the plate was resuspended in sterile saline and adjusted to an OD of 0.1 at 625 nm. The adjusted bacterial suspension was further diluted to target an infecting inoculum of approximately 5.0×10^6−1.0×10^7

https://dx.doi.org/10.1021/acsinfecdis.0c00019
ACS Infect. Dis. 2020, 6, 1378−1388

CFU/mouse. The actual inoculum size varied between 5.5×10^6−1.6×10^6 CFU/thigh and administered via intramuscular injection of (100 μL). Plate counts of the inoculum were performed to confirm inoculum concentration and treatment was initiated 2 h after bacterial challenge.

ETX0282 and CPDP were formulated in 0.5% HPMC/0.1% Tween 80 suspension. meropenem (utilized as a positive control) was solubilized in water for injection. All studies utilized a meropenem dosed at 600 mg/kg q6h subcutaneously as positive control against meropenem sensitive isolates (MIC ≤ 2 μg/mL) and as a negative control against meropenem resistant isolates. For dose arms utilizing a combination of ETX0282 and CPDP, both agents were reconstituted in the same vehicle. All dose concentrations were adjusted to deliver targeted mg/kg doses within a dose volume of 10 mL/kg. Formulation potency was verified by LC/MS/MS.

ETX0282 and CPDP were administered via q6h dose intervals in order to achieve targeted unbound exposures. At 24 h post initiation of therapy, animals were euthanized, tissue samples aseptically collected and homogenized. Bacterial colony enumeration of tissue homogenate was performed by serial dilution on TSA plates which were incubated overnight at 35 °C prior to colony (CFU) counting.

Mouse Oral (ETX0282 and CPDP) Pharmacokinetics. Satellite groups of infected animals were used for pharmacokinetic analysis of ETX1317 and CPD following oral administration of ETX0282 and CPDP. For ETX0282, absolute dose levels of 10, 50, 200, and 400 mg/kg were evaluated. CPDP was evaluated at a single dose level of 50 mg/kg. Three animals were utilized per blood sampling time point with three time points per animal—two submandibular bleeds and one terminal bleed taken via cardiac puncture. Blood samples (50 μL) were collected into K_2EDTA microtainer tubes and process for plasma. Resulting plasma was diluted 1:1 with a solution of SIGMFAST protease inhibitor (10 mg/mL in water), prior to storage at −70 °C. Time points were taken at 0.25, 0.5, 1, 2, 4, and 6 h post-dose.

Rat, Dog, and Monkey Oral (ETX0282) and Intravenous (ETX1317) Pharmacokinetics. Intravenous pharmacokinetics of ETX1317 investigated in jugular vein cannulated male Sprague−Dawley rats (Charles River Laboratories, n = 3/route) at a dose of 10 mg/kg formulated in 0.9% saline. Oral pharmacokinetics of ETX0282 was evaluated at a 10 mg/kg equivalent dose of ETX1317 formulated in 25:75 PEG 400:WFI. The pH of each formulation was verified to fall within a range of 4−7 and were confirmed to be in solution prior to dosing. Potency was verified by LC/MS/MS. Dose volumes were 5 and 10 mL/kg for ETX1317(i.v.) and ETX0282(p.o.), respectively for rats. In both dog (male, 3/route) and monkey (male, 3/route) studies, i.v. and p.o. doses were formulated on 25:75 PEG 400:WFI (pH ∼5) and administered at a dose of ∼1 mg/kg. Dose volume was 1 mL/kg for both routes in dogs and monkeys with the i.v. dose infused over 15 min. For oral doses, gavage tubes were flushed with 10 mL after administration of the dose. i.v. doses were sterile-filtered through 0.22 μm PVDF membrane prior to administration into the cephalic vein.

Blood samples to be processed for plasma using K_2EDTA as an anticoagulant were taken at 0.08, 0.17, 0.25, 0.5, 1, 2, 4, and 8 h (i.v.) and 0.25, 0.5, 1, 2, 4, 8, and 24 h (p.o.) post dose in rats. Blood samples collected into 0.5 mL BD microtainers containing 1.0 mg K_2EDTA were centrifuged in a microfuge for 10 min, plasma pipetted to 96 well cryo tubes, and stored at −80 °C prior to analysis.

Blood sampling (∼1 mL) for dogs and monkeys was carried out via venipuncture of the jugular vein at the following time points:

i.v.: pre-dose, 0.083, 0.25 (prior to end of infusion), 0.5, 1, 1.5, 2, 4, 6, 8, 12, and 24 h post-dose

p.o.: pre-dose, 0.25, 0.5, 1, 1.5, 2, 4, 6, 8, 12, and 24 h post-dose

Blood samples were centrifuged at 3200 rpm for 10 min at approximately 5 °C. Plasma samples (500 μL) were transferred to 96-well plate tubes (MatrixTech, 0.5 mL). An equal amount (500 μL) of SIGMAFAST protease inhibitor solution (1 tablet dissolved in 10 mL distilled water, Sigma-Aldrich Part No. S8820) was added as a preservative to the 96-well plate tubes resulting in a 1:1 dilution. Diluted plasma samples were stored at −80 ± 10 °C.

Urine collection was collected directly into Nalgene bottles placed under metabolism cages with frozen ice packs to chill urine over the collection interval. Urine was collected 0−12, and 12−24 h post-dose. Following collection of each urine sample, the total urine weight was recorded and 3 mL aliquots were retained for LC/MS/MS analysis.

ETX1317 Plasma Protein Binding Determination. Plasma protein binding was determined by rapid equilibrium dialysis. Plasma was freshly prepared from blood samples drawn in to EDTA (anticoagulant) containing tubes. Plasma was prepared using a table-top centrifuge and spun per instruction of the tube manufacturer and specifications (Beckton, Dickinson and Company, Franklin Lakes, NJ) and placed on ice prior to use.

Pooled plasma samples were centrifuged at 2000 rpm (approximately 1400g) for 15 min at 4 °C to remove debris. Approximately 90% of the clear supernatant fraction was transferred to a separate tube. Samples (500 μL) were then spiked with a 100× stock solution 100 μM, 0.5 mM, and 10 mM ETX1317 in DMSO respectively for 1, 5, and 100 μM final concentrations, transferred to the top of the filter chambers, and allowed to equilibrate for 15 min prior to centrifugation. The filtrate tubes were centrifuged at 14000g for 15 min at 4 °C. Next, 50 μL of the filtrate was precipitated with 300 μL of acetonitrile containing 250 ng/mL of carbutamide as the internal standard and the samples were analyzed by LC/MS/MS analysis.

LC/MS/MS Determination of ETX1317, ETX0282, CPD, and CPDP. Calibration standards and Quality Control (QC) were prepared in blank matrices of plasma, urine and MHBII by serial dilution. An aliquot of 50 μL of each calibration standard, QC (diluted separately), and unknown plasma, urine or MHBII samples (diluted separately) were transferred to a 96-deep well plate followed by protein precipitation with 300 μL of crash solution (100% acetonitrile containing 0.1% formic acid and 250 ng/mL of carbutamide (internal standard)). The 96-well plated was then vortexed and centrifuged at 4000 rpm for 5 min and 100 μL of supernatant was transferred for LC-MS/MS analysis.

The plasma, urine, and MHBII concentrations of ETX1317, ETX0282, CPD and CPDP were determined with a non-GLP bioanalytical method using liquid chromatography with mass spectrometric detection (LC/MS/MS), as summarized in Table S4. A calibration curve was constructed using fortified standards and analyzed with the peak area ratios of ETX1317, ETX0282, CPD, and CPDP/carbutamide (internal standard)

https://dx.doi.org/10.1021/acsinfecdis.0c00019
ACS Infect. Dis. 2020, 6, 1378−1388

fitted by linear regression. QC and PK sample concentrations were determined by reference to the calibration curve. The assay had a LLOQ and ULOQ of 5 ng/mL and 5000 ng/mL, respectively, for all analytes.

Pharmacokinetic Analysis. Non-compartmental analysis of time vs concentration data for ETX1317, ETX0282, CPD, and CPDP was completed using WinNonlin 8.1 (Pharsite Corporation, Mountain View CA). The maximum concentration (C_{max}) was the highest observed concentration; T_{max} was the earliest time at which C_{max} occurred; and the elimination half-life was estimated as ln $2/k_{el}$, where k_{el} is the elimination rate constant derived from the slope of the log concentration versus time profile. The area under the concentration−time curve from 0 h to the last time point ($AUC_{0\text{-tlast}}$) was calculated by linear trapezoidal approximation. Clearance (CL) was estimated as Dose/$AUC_{0\text{-tlast}}$ and the steady state volume of distribution ($V_{d,ss}$) was estimated as CL* MRT, where MRT = AUMC/AUC (MRT = mean residence time and AUMC = area under the moment curve). Oral bioavailability (F) was determined from ETX1317 concentrations and normalizing doses to free acid equivalence, where $F = AUC_{p.o.}*(dose_{i.v.})/AUC_{i.v.}*(dose_{p.o.})$.

E_{max} Modeling. Plasma samples from *in vivo* studies and serial media samples from hollow fiber/chemostat experiments were processed and assayed for drug concentration using standard LC/MS/MS methods. The pharmacodynamic results (change in $\log_{10}$ CFU/mL from 0 h) and PK analysis were analyzed using Phoenix WinNonlin 8.1 (Pharsight, Mountain View, CA). The exposure parameters AUC (area under the 24 h concentration−time curve), C_{max} (peak concentration) and %Time > C_T (defined as percent time in a 24 h period where the free drug concentration is at or above the C_T were analyzed for correlation with pharmacodynamic response. A WinNonlin sigmoidal E_{max} model was subsequently used to calculate the PK/PD index that was closely associated with efficacy and its magnitude. The indices most closely associated with efficacy were identified based on dispersion of the data, coefficient of variation in the model calculated parameters, weighted sum of squared residuals and optimization of R^2 values for the relationship.

■ ASSOCIATED CONTENT

Supporting Information

The Supporting Information is available free of charge at https://pubs.acs.org/doi/10.1021/acsinfecdis.0c00019.

> Table S1, ETX1317 PK following oral administration of ETX0282 to nonclinical species; Table S2, cross-species plasma protein binding; Figure S1, plasma concentration vs time PK profiles; Figure S2, CFU burden plots; Table S3, %Time > C_T of 1 μg/mL of a 500 mg equivalent dose of ETX1317 based upon clearance, bioavailability, and absorption rate; and Table S4, LC/MS/MS conditions (PDF)

■ AUTHOR INFORMATION

Corresponding Author

John O'Donnell − *Entasis Therapeutics, Waltham, Massachusetts 02451, United States;* orcid.org/0000-0001-5502-8738; Email: john.odonnell@entasistx.com

Authors

Angela Tanudra − *Entasis Therapeutics, Waltham, Massachusetts 02451, United States*

April Chen − *Entasis Therapeutics, Waltham, Massachusetts 02451, United States*

Daniel Hines − *Entasis Therapeutics, Waltham, Massachusetts 02451, United States*

Ruben Tommasi − *Entasis Therapeutics, Waltham, Massachusetts 02451, United States;* orcid.org/0000-0002-1573-7422

John Mueller − *Entasis Therapeutics, Waltham, Massachusetts 02451, United States;* orcid.org/0000-0001-9368-4015

Complete contact information is available at: https://pubs.acs.org/10.1021/acsinfecdis.0c00019

Notes

The authors declare the following competing financial interest(s): All co-authors are employees of Entasis Therapeutics.

■ ACKNOWLEDGMENTS

This work was supported by the Cooperative Agreement Number IDSEP160030 from ASPR/BARDA and by awards from Wellcome Trust and Germany's Federal Ministry of Education and Research (BMBF), as administrated by CARB-X. The content is solely the responsibility of the authors and does not necessarily represent the official views of the Department of Health and Human Services Office of the Assistant Secretary for Preparedness and Response, other funders, or CARB-X. Animal efficacy studies were supported by Neosome Life Sciences, Lexington MA.

■ REFERENCES

(1) Paterson, D. L. (2006) Resistance in Gram-Negative Bacteria: Enterobacteriaceae. *Am. J. Med. 119*, S20−S28.

(2) Iredell, J., Brown, J., and Tagg, K. (2016) Antibiotic resistance in Enterobacteriaceae: mechanisms and clinical implications. *BMJ. 2016*, 352.

(3) Pitout, J. D. (2008) Multiresistant Enterobacteriaceae: new threat of an old problem. *Expert Rev. Anti-Infect. Ther. 6* (5), 657−669.

(4) Hooper, D. C. (2001) Emerging Mechanisms of Fluoroquinolone Resistance. *Emerging Infect. Dis. 7* (2), 337−341.

(5) Redgrave, L. S., Sutton, S. B., Webber, M. A., and Piddock, L. J. V. (2014) Fluoroquinolone resistance: mechanisms, impact on bacteria, and role in evolutionary success. *Trends Microbiol. 22* (8), 438−445.

(6) Bouchillon, S., Hoban, D. J., Badal, R., and Hawser, S. (2012) Fluoroquinolone resistance among gram-negative urinary tract pathogens: global smart program results, 2009−2010. *Open Microbiol. J. 6*, 74−78.

(7) Dalhoff, A. (2012) Global Fluoroquinolone Resistance Epidemiology and Implications for Clinical Use. *Interdiscip. Perspect. Infect. Dis. 2012*, 1−37.

(8) Johnson, L., Sabel, A., Burman, W. J., Everhart, R. M., Rome, M., MacKenzie, T. D., Rozwadowski, J., Mehler, P. S., and Price, C. S. (2008) Emergence of fluoroquinolone resistance in outpatient urinary Escherichia coli isolates. *Am. J. Med. 121*, 876−884.

(9) Drawz, S. M., Papp-Wallace, K. M., and Bonomo, R. A. (2014) New β-lactamase inhibitors: a therapeutic renaissance in an MDR world. *Antimicrob. Agents Chemother. 58*, 1835−1846.

(10) Bear, D. M., Turck, M., and Petersdorf, R. G. (1970) Ampicillin. *Med. Clin. North Am. 54* (5), 1145−1159.

(11) Ronald, A. R., Jagdis, F. A., Harding, G. K. M., Hoban, S. A., Muir, P. L., and Gurwith, M. J. (1977) Amoxicillin Therapy of Acute

Urinary Infections in Adults. *Antimicrob. Agents Chemother. 11* (5), 780−784.
(12) Itokazu, G. S., and Danziger, L. H. (1991) Ampicillin-Sulbactam and Ticarcillin-Clavulanic Acid: A Comparison of Their *In Vitro* Activity and Review of Their Clinical Efficacy. *Pharmacotherapy 11*, 382S−414S.
(13) White, A. R., Kaye, C., Poupard, J., Pypstra, R., Woodnutt, G., and Wynne, B. (2004) Augmentin® (amoxicillin/clavulanate) in the treatment of community-acquired respiratory tract infection: a review of the continuing development of an innovative antimicrobial agent. *J. Antimicrob. Chemother. 53* (Suppl. S1), 3i−20.
(14) Bretschneider, B., Brandsch, M., and Neubert, R. (1999) Intestinal transport of beta-lactam antibiotics: analysis of the affinity at the H^+/peptide symporter (PEPT1), the uptake into Caco-2 cell monolayers and the transepithelial flux. *Pharm. Res. 16*, 55−61.
(15) Rawat, D., and Nair, D. (2010) Extended-spectrum β-lactamases in Gram Negative Bacteria. *J. Glob Infect Dis. 2* (3), 263−274.
(16) Rishi, H., Dhillon, P., and Clark, J. (2012) ESBLs: A Clear and Present Danger? *Critical Care Research and Practice 2012*, 1−11.
(17) Paterson, D. L., and Bonomo, R. A. (2005) Extended-spectrum beta-lactamases: a clinical update. *Clin. Microbiol. Rev. 18* (4), 657−686.
(18) Shirley, M. (2018) Ceftazidime-Avibactam: A Review in the Treatment of Serious Gram-Negative Bacterial Infections. *Drugs 78*, 675−692.
(19) Hecker, S. J., Reddy, K. R., Totrov, M., Hirst, G. C., Lomovskaya, O., Griffith, D. C., King, P., Tsivkovski, R., Sun, D., Sabet, M., Tarazi, Z., Clifton, M. C., Atkins, K., Raymond, A., Potts, K. T., Abendroth, J., Boyer, S. H., Loutit, J. S., Morgan, E. E., Durso, S., and Dudley, M. N. (2015) Discovery of a Cyclic Boronic Acid β-Lactamase Inhibitor (RPX7009) with Utility vs Class A Serine Carbapenemases. *J. Med. Chem. 58* (9), 3682−92.
(20) Cyriac, J. M., and James, E. (2014) Switch over from intravenous to oral therapy: A concise overview. *J. Pharmacol. Pharmacother. 5* (2), 83−87.
(21) Miller, A. A., Shapiro, A. B., McLeod, S. M., Carter, N. M., Moussa, S. H., Tommasi, R., and Mueller, J. P. (2020) *In vitro* Characterization of ETX1317, a novel, broad-spectrum β-lactamase inhibitor that restores and enhances β-lactam activity against multidrug resistant *Enterobacteriaceae*, including carbapenem-resistant strains. *ACS Infect. Dis.*, DOI: 10.1021/acsinfecdis.0c00020, following paper in this issue.
(22) Bergan, T. (1987) Pharmacokinetic Properties of the Cephalosporins. *Drugs 34* (Suppl 2), 89.
(23) Borin, M. T., Hughes, G. S., Patel, R. K., Royer, M. E., and Cathcart, K. S. (1991) Pharmacokinetic and tolerance studies of cefpodoxime after single- and multiple-dose oral administration of cefpodoxime proxetil. *J. Clin. Pharmacol. 31*, 1137−1145.
(24) Borin, M. T. (1991) A review of the pharmacokinetics of cefpodoxime proxetil. *Drugs 42* (Suppl 3), 13−21.
(25) Quintiliani, R., Nightingale, C. H., and Freeman, C. D. (1994) Pharmacokinetic and Pharmacodynamic Considerations in Antibiotic Selection, with Particular Attention to Oral Cephalosporins. *Infectious Diseases in Clinical Practice 3* (1), 1−7.
(26) Turnidge, J. D. (1998) The Pharmacodynamics of β-Lactams. *Clin. Infect. Dis. 27* (1), 10−22.
(27) CLSI (2018) *M100: Performance Standards for Antimicrobial Susceptibility Testing*, 28th ed., Clinical Laboratory Standards Institute, Wayne, PA.
(28) Blaser, J., and Zinner, S. H. (1987) *In vitro* models for the study of antibiotic activities. *Prog. Drug Res. 31*, 349−381.
(29) Bulitta, J. B., Hope, W. W., Eakin, A. E., Guina, T., Tam, V. H., Louie, A., Drusano, G. L., and Hoover, J. L. (2019) Generating robust and informative nonclinical in vitro and in vivo bacterial infection model efficacy data to support translation to humans. *Antimicrob. Agents Chemother. 63*, e02307−18.
(30) Tam, V. H., Louie, A., Fritsche, T. R., Deziel, M., Liu, W., Brown, D. L., Deshpande, L., Leary, R., Jones, R. N., and Drusano, G. L. (2007) Impact of Drug-Exposure Intensity and Duration of Therapy on the Emergence of Staphylococcus aureus Resistance to a Quinolone Antimicrobial. *J. Infect. Dis. 195* (12), 1818−1827.
(31) Cadwell, J. J. S. (2012) The Hollow Fiber Infection Model for Antimicrobial Pharmacodynamics and Pharmacokinetics. *Adv. Pharmacoepidemiol. Drug Saf. 01* (S1), 007.
(32) Grasso, S., Meinardi, G., De Carneri, I., and Tamassia, V. (1978) New *in vitro* model to study the effect of antibiotic concentration and rate of elimination on antibacterial activity. *Antimicrob. Agents Chemother. 13* (4), 570−576.
(33) Louie, A., Castanheira, M., Liu, W., Grasso, C., Jones, R. N., Williams, G., Critchley, I., Thye, D., Brown, D., VanScoy, B., Kulawy, R., and Drusano, G. L. (2012) *Antimicrob. Agents Chemother. 56* (1), 258−270.
(34) Nichols, W. W., Newell, P., Critchley, I. A., Riccobene, T., and Das, S. (2018) Avibactam pharmacokinetic/pharmacodynamic targets. *Antimicrob. Agents Chemother. 62*, e02446−17.
(35) Singh, R., Kim, A., Tanudra, M. A., Harris, J. J., McLaughlin, R. E., Patey, S., O'Donnell, J. P., Bradford, P. A., and Eakin, A. E. (2015) Pharmacokinetics/pharmacodynamics of a β-lactam and β-lactamase inhibitor combination: a novel approach for aztreonam/avibactam. *J. Antimicrob. Chemother. 70* (9), 2618−2626.
(36) VanScoy, B., Mendes, R. E., Nicasio, A. M., Castanheira, M., Bulik, C. C., Okusanya, O. O., Bhavnani, S. M., Forrest, A., Jones, R. N., Friedrich, L. V., Steenbergen, J. N., and Ambrose, P. G. (2013) PKPD of tazobactam in combination with ceftolozane in an *in vitro* infection model. *Antimicrob. Agents Chemother. 57* (6), 2809−2814.
(37) Nicasio, A. M., VanScoy, B. D., Mendes, R. E., Castanheira, M., Bulik, C. C., Okusanya, O. O., Bhavnani, S. M., Forrest, A., Jones, R. N., Friedrich, L. V., Steenbergen, J. N., and Ambrose, P. G. (2016) Pharmacokinetics-pharmacodynamics of tazobactam in combination with piperacillin in an *in vitro* infection model. *Antimicrob. Agents Chemother. 60*, 2075−2080.
(38) VanScoy, B. D., Tenero, D., Turner, S., Livermore, D. M., McCauley, J., Conde, H., Bhavnani, S. M., Rubino, C. M., and Ambrose, P. G. (2017) Pharmacokinetics-pharmacodynamics of tazobactam in combination with cefepime in an *in vitro* infection model. *Antimicrob. Agents Chemother. 61*, e01052−17.
(39) Andes, D., and Craig, W. A. (2005) Treatment of infections with ESBL-producing organisms: pharmacokinetic and pharmacodynamic considerations. *Clin. Microbiol. Infect. 11*, 10−17.
(40) DeRyke, C., and Nicolau, D. (2007) Is all free time above the minimum inhibitory concentration the same: implications for β-lactam in vivo modeling. *Int. J. Antimicrob. Agents 29*, 341−343.
(41) Kidd, J. M., Abdelraouf, K., and Nicolau, D. P. (2020) Efficacy of human-simulated bronchopulmonary exposures of cefepime, zidebactam and the combination (WCK 5222) against MDR *Pseudomonas aeruginosa* in a neutropenic murine pneumonia model. *J. Antimicrob. Chemother. 75* (1), 149−155.
(42) Durand-Réville, T., Comita-Prevoir, J., Zhang, J., Wu, X., May-Dracka, T. L., Romero, J., Wu, F., Chen, A., Shapiro, A. B., Carter, N. M., McLeod, S. M., Giacobbe, R. A., Verheijen, J. C., Lahiri, S. D., Sacco, M. D., Chen, Y., O'Donnell, J. P., Miller, A. A., Mueller, J. P., and Tomassi, R. (2020) Discovery of ETX0282, an Orally Available Diazabicycloocta(no)ne Inhibitor of Class A, C and D Serine β-lactamases. *J. Med. Chem.*, submitted.
(43) O'Donnell, J., Miller, A., Shankaran, H., Ferguson, D., Newman, J., Tommasi, R., and Mueller, J. (2016) Poster 2245. Human Dose Projection of ETX2514/Sulbactam Combination for Use in the Treatment of Infections Caused by *Acinetobacter baumannii*. IDweek 2016, New Orleans, LA.
(44) Merdjan, H., Tarral, A., Das, S., and Li, J. (2017) Phase 1 Study Assessing the Pharmacokinetic Profile and Safety of Avibactam in Patients with Renal Impairment. *J. Clin. Pharmacol. 57*, 211−218.
(45) O'Donnell, J., Preston, R. A., Mamikonyan, G., Stone, E., and Isaacs, R. (2019) Pharmacokinetics, safety, and tolerability of intravenous durlobactam and sulbactam in subjects with renal impairment and healthy matched control subjects. *Antimicrob. Agents Chemother. 63*, e00794−19.

(46) Huh, Y., Smith, D. E., and Feng, M. R. (2011) Interspecies scaling and prediction of human clearance: Comparison of small and macromolecule drugs. *Xenobiotica 41*, 972−987.
(47) Paine, S. W., Menochet, K., Denton, R., McGinnity, D., and Riley, R. (2011) Prediction of human clearance from preclinical species for a diverse set of drugs that exhibit both active secretion and net reabsorption. *Drug Metab. Dispos. 39*, 1008−1013.
(48) Gerber, A. U., Craig, W. A., Brugger, H. P., Feller, C., Vastola, A. P., and Brandel, J. (1983) Impact of dosing intervals on activity of gentamycin and ticarcillin against *Pseudomonas aeruginosa* in normal and granulocytopenic mice. *J. Infect. Dis. 147*, 910−17.
(49) Gudmundsson, S., Vogelman, B., and Craig, W. A. (1986) The in-vivo postantibiotic effect of imipenem and other new antimicrobials. *J. Antimicrob. Chemother. 18* (Suppl. E), 67−73.

https://dx.doi.org/10.1021/acsinfecdis.0c00019
ACS Infect. Dis. 2020, 6, 1378−1388